



ELSEVIER

Contents lists available at ScienceDirect

Materials Letters

journal homepage: www.elsevier.com/locate/matlet

Pseudopartial wetting of WC/WC grain boundaries in cemented carbides



B.B. Straumal^{a,b,c,d,*}, I. Konyashin^{c,e}, B. Ries^e, A.B. Straumal^{a,c}, A.A. Mazilkin^{a,b},
K.I. Kolesnikova^{a,c}, A.M. Gusak^f, B. Baretzky^b

^a Institute of Solid State Physics, Russian Academy of Sciences, Chernogolovka, Russia

^b Karlsruhe Institut für Technologie, Institut für Nanotechnologie, Eggenstein-Leopoldshafen, Germany

^c National University of Science and Technology "MISIS", Moscow, Russia

^d Moscow Institute of Physics and Technology (State University), Dolgoprudny, Russia

^e Element Six GmbH, Technical Development Centre, Burghaun, Germany

^f Department of Theoretical Physics, Cherkasy National University, Cherkasy, Ukraine

ARTICLE INFO

Article history:

Received 13 January 2015

Accepted 6 February 2015

Available online 16 February 2015

Keywords:

Phase transitions

Cemented carbides

Grain boundaries

Wetting

ABSTRACT

WC–Co cemented carbides are metal–ceramic composites consisting of a ceramic phase, tungsten carbide, and a cobalt binder. The key to the exceptional properties of cemented carbides is the optimal combination of hardness and wear-resistance of WC grains, and toughness and ductility of the Co-based matrix. However, only the minority of WC/WC GBs are completely wetted by Co melt during the liquid phase sintering. We observed for the first time that other WC/WC GBs are not partially wetted and, therefore, “dry”. They are pseudopartially wetted, namely they have the high contact angle with cobalt binder and, nevertheless, contain the 2–3 nm thin uniform Co-rich layer.

© 2015 Elsevier B.V. All rights reserved.

1. Introduction

WC–Co cemented carbides are metal–ceramic composites consisting of a ceramic phase, tungsten carbide, and a cobalt binder. They are broadly used in various industrial applications and almost in each household, for example, as masonry drill bits, due to their unique combination of high hardness, wear-resistance, toughness and strength. Since their discovery in Germany in the 1920s, WC–Co cemented carbides did not dramatically change. The main improvements were related to varying WC grain size, Co content and employing inhibitors of WC grain growth during liquid phase sintering [1,2]. The key to the exceptional properties of cemented carbides is the optimal combination of hardness and wear-resistance of WC grains, and toughness and ductility of the Co-based matrix. Also, the presence of a carbide skeleton, or so to say “pseudo-skeleton” of WC grains in the carbide microstructure appears to play a very important role with respect to obtaining the unique combination of hardness and fracture toughness of cemented carbides. The skeleton can be designated as the “pseudo-skeleton”, based on the fact that almost all the WC–WC grain boundaries are known to comprise very thin Co interlayers of the order of from nearly one atomic monolayer to several nanometers

[3–5]. In this respect, the wetting of boundaries between WC grains by the Co melt during liquid phase sintering is the key issue. It is because pure WC/WC grain boundaries (GBs) not comprising the Co interlayers should be quite brittle. It is well known that the wettability of WC by liquid Co examined by the method of a lying droplet is complete and the wetting angle of a droplet of liquid Co on the surface of WC is equal to 0 at temperatures of 1400–1500 °C [6,7].

Nevertheless, the presence of the “pseudo-skeleton” of WC grains in the cemented carbide microstructure clearly indicates that WC–WC GBs are characterized by various contact angles with the cobalt-based binder and only very few angles are equal to 0. Therefore, there is a contradiction between the fact of complete wetting of WC by the liquid Co droplet on the one hand, and the contact angles between WC–WC GBs and the Co-based binder different from 0 in the carbide microstructure on the other hand. This contradiction was mentioned as early as in 1972 by Warren and Waldron [8]. The goal of this paper is to investigate the nature of the Co-based interlayers in the WC/WC GBs in cemented carbides and explain the apparent contradiction mentioned above.

2. Experimental

Ultra-coarse WC–Co cemented carbides were produced according to the procedure described in Refs. [9–12]. The WC powder (MAS 3000-5000, H.C. Starck) was milled with 10 wt% Co in an

* Correspondence to: Institute of Solid State Physics, Russian Academy of Sciences, Chernogolovka, Moscow district, 142432 Russia. Tel.: +7 916 6768673; fax: +7 499 2382326.

E-mail address: straumal@issp.ac.ru (B.B. Straumal).

attritor-mill for 1 h in hexane with 2 wt% paraffin wax down to the particle size of 3–10 μm . Samples were pressed and liquid-phase sintered at 1380 $^{\circ}\text{C}$ for 75 min (45 min vacuum+30 min hot isostatic pressing at 4 MPa in argon). After sintering, samples were embedded in resin and then mechanically ground and polished, using 1 μm diamond paste in the last polishing step, to obtain metallurgical cross-sections for the metallographic study. After etching in the Murakami reagent, the cross-sections were investigated by means of optical microscopy and scanning electron microscopy (SEM). For comparison the complete GB wetting in Cu–4 wt% In alloy has been investigated as well (details see in Refs. [13,14]). SEM investigations were carried out on a Tescan Vega TS5130 MM microscope equipped with the LINK energy-dispersive spectrometer produced by Oxford Instruments. Light microscopy was performed using a Neophot-32 light microscope equipped with a 10 Mpix Canon Digital Rebel XT camera. A quantitative analysis of the wetting transition was performed adopting the following criterion: every boundary between WC was considered to be completely wetted by the Co-based phase only when a macroscopic layer of the Co-based binder (of the order of least 1 μm) can be measured by SEM (Fig. 1c, arrow with letter A); if such a layer appeared to be interrupted, the GB was regarded as incompletely wetted (Fig. 1c, arrow with letter B). The contact angles θ were measured simultaneously for all GBs. For the GBs completely covered by a liquid phase the $\theta=0^{\circ}$ value was assigned. At least 300 GBs were analyzed at each temperature. Typical micrograph obtained by SEM is shown in Fig. 1. Transmission

electron microscopy (TEM, HRTEM, STEM, EDXS) studies were carried out on the TECNAI microscope.

3. Results and discussion

Fig. 1a shows microstructure of the Cu–4 wt% In alloy characterized by the complete GB wetting. It can be seen that as a result of grain growth by the dissolution-precipitation mechanism the large Cu grains (appear black) grow in such a way that they adjust with each other leaving relatively thick In-rich interlayers (appear white) among them. These interlayers have a thickness of about several microns. In contrast to that, in the microstructure of the conventional WC–Co grade shown in Fig. 1b the growing WC grains do not adjust with each other resulting in the formation of the “pseudo-skeleton” mentioned above. The microstructure of the carbide sample examined in the present work is shown in Fig. 1c. Fig. 2 shows the histogram indicating the share of WC/WC grain boundaries having a certain contact angle with the Co-based binder. There are very few contact angles equal to 0 ($\theta=0^{\circ}$) corresponding to the complete GB wetting. Fig. 3a shows the Z-contrast image obtained by HAADF STEM in the contact area between two WC grains (bright) and the grain of Co-based binder (dark, removed during the preparation of TEM sample). The EDS profile of Co concentration across WC/WC GB shown in Fig. 3b demonstrates that this grain boundary comprises a thin Co-based layer of nearly 5–7 nm (white line in Fig. 3a). The position of respective line profile is shown in Fig. 3a.

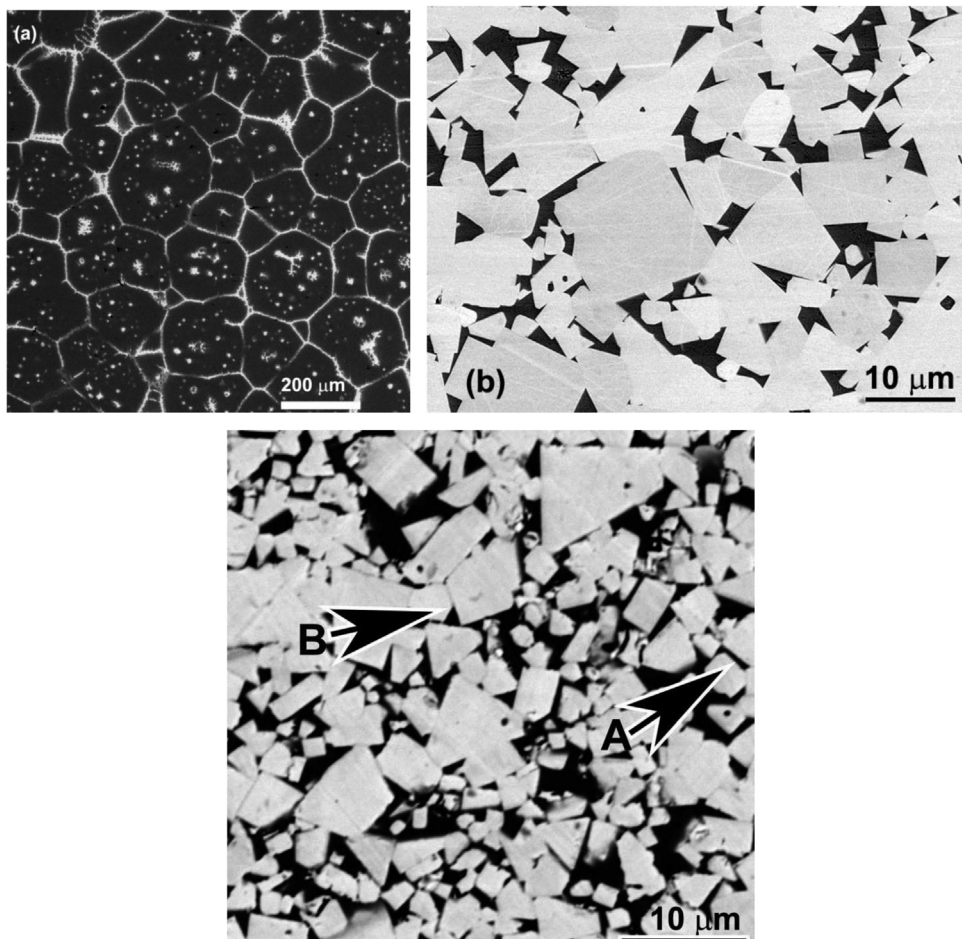


Fig. 1. SEM micrographs of microstructures of (a) Cu–4 wt% In annealed at 990 $^{\circ}\text{C}$ (complete GB wetting) (b) conventional industrial ultra-coarse WC–Co cemented carbide (very few WC/WC–binder contact angles are equal to 0°), and (c) cemented carbide examined in the present work after liquid-phase sintering at 1380 $^{\circ}\text{C}$. (A) WC/WC GB completely wetted by the Co-rich melt, zero contact angle. (B) WC/WC GB incompletely wetted by the melt, non-zero contact angle.

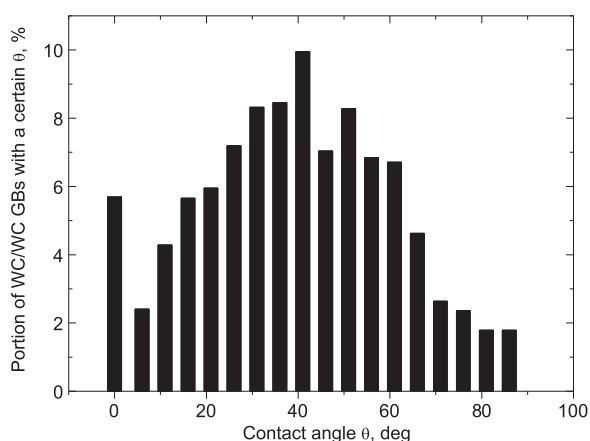


Fig. 2. Histogram showing the the portion of WC/WC grain boundaries having a certain contact angle with the Co-based binder.

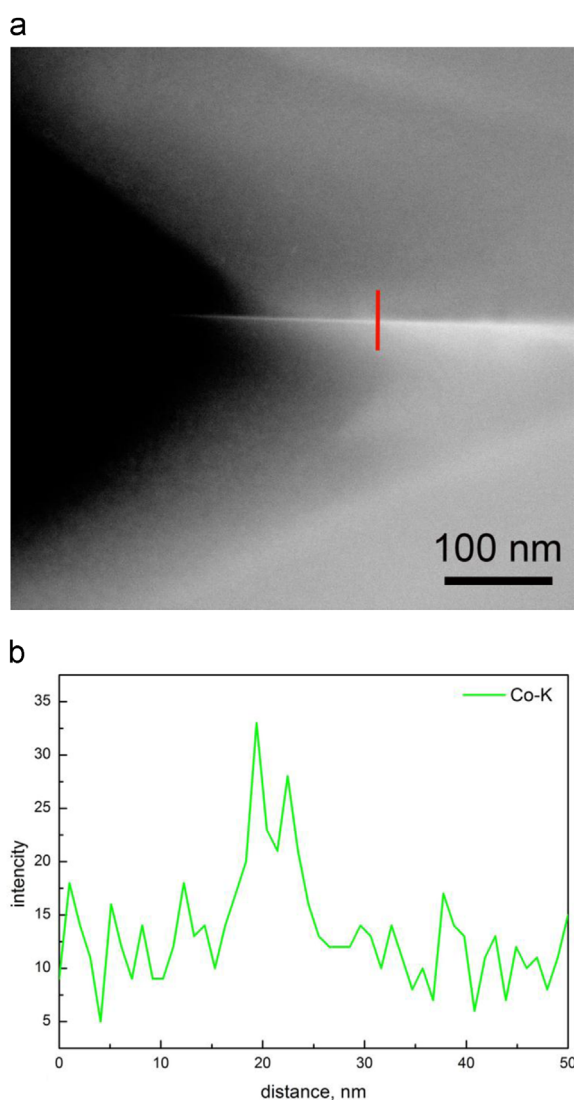


Fig. 3. (a) STEM HAADF image showing the contact area between two WC grains (bright) and the grain of Co-based binder (dark, removed by the preparation of TEM sample). WC/WC grain boundary contains the 5–7 nm thin layer of Co-rich phase (white). (b) EDS profile of Co concentration across WC/WC GB. The position of respective line profile is shown in a.

In order to understand the special features of the cemented carbide microstructure, let us consider the droplet of a liquid phase between two solid grains in a partially melted two-

multicomponent polycrystal. If a liquid droplet partially wets (PW) the boundary between two solid grains, then $\sigma_{gb} = 2\sigma_{sl}\cos\theta$, where σ_{gb} is the free energy of a grain boundary, σ_{sl} is the free energy of solid/liquid interface, and θ is the contact angle. The GB which is not covered by the liquid droplets remains dry and contains only the adsorbed atoms with coverage below one monolayer. In this case the GB can exist in the equilibrium contact with the liquid phase (GBs marked with a letter A in Fig. 1a). In the case of complete wetting $\sigma_{gb} > 2\sigma_{sl}$, the contact angle is zero, and liquid spreads over the free surface or between grains. In this case the GB separating the grains is completely substituted by the liquid phase which has macroscopic (arbitrary) thickness of at least several hundreds of nanometers (GBs marked with a letter B in Fig. 1a). If the condition of complete GB wetting is fulfilled, the thick layer of Co-based binder separates the neighbouring WC grains even if they are strongly faceted (see for example GBs marked by arrow with a letter A in Fig. 1c). The transition from incomplete to complete GB wetting proceeds at a certain T_w if the energy of two solid–liquid interfaces $2\sigma_{sl}$ becomes lower than the GB energy $\sigma_{GB} > 2\sigma_{sl}$. Cahn [15] and Ebner and Saam [16] first showed that the (reversible) transition from incomplete to complete wetting can proceed with increasing temperature, and that it is a true surface phase transformation. The GB wetting temperatures T_w , depend both on GB energy and solid–liquid interfacial energy which, in turn, depend on the crystallography of these interfaces [17–21].

In the case of complete wetting (CW) $\sigma_{gb} > 2\sigma_{sl}$, the contact angle is zero, and liquid spreads between grains, which is clearly seen in the microstructure of the Cu–4 wt% In alloy shown in Fig. 1a. What happens, if the amount of liquid is small and GB area is large? In this case the liquid spreads until both solid grains or solid and gas begin to interact with each other through the liquid layer. The liquid forms a “pancake” with a thickness e_s about 2–5 nm [22,23] $e_s = (A/4\pi S)^{1/2}$, where $S = \sigma_{gb} - 2\sigma_{sl}$ is the spreading coefficient on a strictly “dry” GB and A is the Hamaker constant [16]. In case of complete wetting $A > 0$ and $S > 0$ [23]. Such “pancake” between the grains is formed by the deficit of a wetting phase, i.e. in the $\alpha + L$ two-phase area of a phase diagram, but very close to the solidus line. The thin “pancake” is very similar to the observed in our cemented carbide sample and presented in Fig. 3. However, in our case the amount of Co-binder is high and one cannot speak about deficit of liquid phase. The share of completely wetted WC/WC GBs with zero contact angle is also quite low (Fig. 2), although the contact angle θ between WC/WC GB covered by the thin Co layer is about 90° (Fig. 3), i.e. far away from zero. What is the reason for the coexistence of thin Co-rich GB layer between WC grains and high contact angle θ ?

In the majority of cases the direct transition occurs from partial into complete wetting, for example by increasing temperature [21,24,25] or decreasing pressure [26]. However, in some cases the state of pseudopartial wetting (PPW) occurs between partial and complete wetting. In this case the contact angle $\theta > 0$, the liquid droplet does not spread over the substrate, but a thin (few nm) precursor film forms around the droplet and separates the substrate and gas or two abutting grains. Such a precursor film is very similar for the liquid “pancake” in case of complete wetting and deficit of the liquid phase. This case is designated as “pseudopartial wetting” and becomes possible when $A < 0$ and $S > 0$ [23]. In case of pseudopartial wetting the precursor film exists together with liquid droplets, and in case of complete wetting the droplets disappear forming the “pancake”.

The sequence of discontinuous $PW \leftrightarrow PPW$ and continuous $PPW \leftrightarrow CW$ transitions was observed for the first time in the alkanes/water mixture [27]. The first direct measurement of the contact angle in the intermediate wetting state (PPW) was performed in the sequential-wetting scenario of hexane on salt brine [28]. Later on the formation of Pb, Bi and binary Pb–Bi

precursors surrounding liquid or solidified droplets was observed on the surface of solid copper [29]. The pseudopartial wetting was observed also for other GBs, for example [30].

To our minds, just the phenomenon of PPW can explain the special features of the cemented carbide microstructure and apparent contradiction between the fact of complete wetting of WC by a liquid Co droplet and the contact angles between the WC–WC GBs and Co-based binder different from 0. During the experiments on spreading of the liquid Co droplet over WC there are three boundaries: liquid–gas, solid–gas and liquid–solid. In this case the interface energy in the systems WC/gas and (liquid Co)/gas is presumably significantly higher than that between solid WC and liquid Co. As a result, the liquid Co droplet spreads over the surface of WC resulting in the fact that the wetting angle of liquid Co on the surface of WC is equal to 0, thus indicating the complete surface wetting. In the initial stage of sintering of carbide green bodies when the liquid phase just forms, there are also three boundaries: liquid–gas, solid–gas and liquid–solid. In this case, the wetting of WC by liquid Co is complete and the carbide densification to the full density occurs very fast resulting in the elimination of the liquid–gas and solid–gas interfaces. When only the solid–liquid interface remains in the sintered carbide body after the completion of the initial sintering stage, the solid–liquid interface is presumably characterized by pseudopartial wetting. Large WC grains growing at the expense of dissolving fine WC grains do not arrange with each other leaving a thin binder layers among them, as it would be in the case of complete wetting. Instead of that, they grow together forming the “pseudo-skeleton” comprising very thin precursor films of a Co-based alloy of several nanometers in thickness. It can be expected that the composition of the precursor films is significantly different from that of the binder phase in the macroscopic interlayers among WC grains. Particularly, it is well known that the Co-based alloy of the thin Co interlayers located at WC–WC interfaces cannot be leached off from the fully sintered carbide body [31]. Also, almost all the WC grain growth inhibitors except for Ta are known to segregate at the WC–WC interfaces being dissolved in the Co-based precursor films [5].

4. Conclusions

The key to the exceptional properties of cemented carbides is the optimal combination of hardness and wear-resistance of WC grains, and toughness and ductility of the Co-based matrix. We observed that only the minority of WC/WC GBs are completely wetted by thick Co layers. However, we observed for the first time that other WC/WC GBs are not partially wetted and, therefore, “dry”. They are pseudo-partially wetted, namely they have the high contact angle with cobalt binder and, nevertheless, contain the 2–3 nm thin uniform Co-rich layer.

Acknowledgments

The work was partially supported by the Russian Foundation for Basic Research (Grants 13-08-90422, 14-48-03598, and 14-42-03621), Government of Moscow Region, (grants 14-48-03598, and 14-42-03621), Ukrainian Fundamental Research State Fund (Grant Φ 53/112-2013), Ministry of Education and Science of the Russian Federation in the framework of Increase Competitiveness Program of MISiS, programme “New materials” of RAS, European Community’s Seventh Framework Programme (FP7-PEOPLE-2013-IRSES) under EC-GA no. 612552 and Karlsruhe Nano Micro Facility operated by the Karlsruhe Institute of Technology.

References

- [1] Bose A. *Int J Powder Metall* 2011;47(2):31–50.
- [2] Kolaska H. *Powder Met Int* 1992;24:311–20.
- [3] Sharma NK, Wards ID, Fraser HL, Williams WS. *J Am Ceram Soc* 1980;63:194–6.
- [4] Henjered A, Helsing M, Nouet G, Dubon A, Laval J. *Mater Sci Technol* 1994;2:847–55.
- [5] Weidow J, Andr n H-O. *Int J Refract Met Hard Mater* 2011;29:38–43.
- [6] Gurland J, Norton L. *J Met* 1952;4:1045–50.
- [7] Ramqvist L. *Int J Powder Met* 1965;1:2–20.
- [8] Warren R, Waldron MB. *Powder Metall* 1972;30:166–80.
- [9] Konyashin I, Cooper R, Ries B. Cemented carbide in particular for cutting stone, concrete and asphalt. German Patent 10258537; 2006.
- [10] Konyashin I, Cooper R, Ries B. Cemented carbide in particular for cutting stone, concrete and, asphalt [EP1520056]; 2004.
- [11] Konyashin I, Ries B, Lachmann F. Cemented carbide material [WO2012/130851]; 2012.
- [12] Konyashin I, Sch fer F, Cooper R, Mayer J, Weirich T. *Int J Refract Met Hard Mater* 2005;23:225–32.
- [13] Straumal AB, Bokstein BS, Petelin AL, Straumal BB, Baretzky B, Rodin AO, et al. *J Mater Sci* 2012;47:8336–43.
- [14] Straumal BB, Kogtenkova OA, Kolesnikova KI, Straumal AB, Bulatov MF, Nekrasov AN. *JETP Lett* 2014;100:535–9.
- [15] Cahn JW. *J Chem Phys* 1977;66:3667–74.
- [16] Ebner C, Saam WF. *Phys Rev Lett* 1977;38:1486–9.
- [17] Straumal BB, Klingner LM, Shvindlerman LS. *Acta Metall* 1984;32:1355–64.
- [18] Straumal BB, Shvindlerman LS. *Acta Metall* 1985;33:1735–49.
- [19] Straumal BB, Polyakov SA, Mittemeijer EJ. *Acta Mater* 2006;54:167–72.
- [20] Sch llhammer J, Baretzky B, Gust W, Mittemeijer E, Straumal B. *Interface Sci* 2001;9:43–53.
- [21] Straumal B, Muschik T, Gust W, Predel B. *Acta Metal Mater* 1992;40:939–45.
- [22] Luo J. *Crit Rev Solid State Mater Sci* 2007;32:67–109.
- [23] Brochard-Wyart F, di Meglio JM, Qu r  D, de Gennes PG. *Langmuir* 1991;7:335–8.
- [24] Straumal BB, Gornakova AS, Kogtenkova OA, Protasova SG, Sursaeva VG, Baretzky B. *Phys Rev B* 2008;78:054202.
- [25] Straumal BB, Zieba P, Gust W. *Int J Inorg Mater* 2001;3:1113–5.
- [26] Straumal B, Rabkin E, Lojkowski W, Gust W, Shvindlerman LS. *Acta Mater* 1997;45:1931–40.
- [27] Bertrand E, Dobbs H, Broseta D, Indekeu J, Bonn D, Meunier J. *Phys Rev Lett* 2000;85:1282–5.
- [28] Rafa  S, Bonn D, Bertrand E, Meunier J. *Phys Rev Lett* 2004;92:245701.
- [29] Moon J, Garoff S, Wynblatt P, Suter R. *Langmuir* 2004;20:402–8.
- [30] Straumal BB, Sauvage X, Baretzky B, Mazilkin AA, Valiev RZ. *Scr Mater* 2014;70:59–62.
- [31] Kreimer GS. *Strength of Hard Alloys*. New York, USA: Consultants Bureau; 1968.